CORROSION SCIENCE AND TECHNOLOGY, Vol.23, No.6(2024), pp.527~537 pISSN 1598-6462 / eISSN 2288-6524
[Research Paper] DOI: https://doi.org/10.14773/cst.2024.23.6.527

Measurement of Levels of Dross Intermetallic Particles in 55%Al-Zn Alloy Based Metal Coating Bath by Pressure Filtration Technique

Nega Setargew[1,†], Greg Harris[2], Uyen Kieu[2], Nghia Truong[2], and Jaka Prakasha[3]

[1]*BlueScope Innovation Lab, Port Kembla, NSW 2505, Australia*
[2]*Nippon Steel-BlueScope Vietnam, Ma Phut, Vietnam*
[3]*Nippon Steel- BlueScope Indonesia, Cilegon, Indonesia*

(Received May 31, 2024; Revised August 06, 2024; Accepted August 07, 2024)

A pressure filtration technique was used to measure levels of dross intermetallic compound particles (IMCs) to assess overall metal cleanliness of 55%Al-Zn alloy-based metal coating bath. The weight of molten metal passing through a micro-filter was measured at constant pressure and temperature using a Prefil-Footprinter, a portable inclusion analyser. Fundamental cake filtration theory was applied to analyse Prefil data. Inverse average filtration rate (t/V) and dt/dV was plotted as a function of cumulative filtrate volume (V) to generate filtrations curves. Cake mode filtration parameters were determined from linearized plots of a constant pressure filtration equation ($\frac{t}{V}=\frac{\mu\alpha_{av}C}{2A^2\Delta P}+\frac{\mu R_m}{A\Delta P}$) The linear diagram in the dt/dV form was used to assess deviations due to secondary effects. The IMC mass captured/unit volume of filtrate was calculated based on chemical analysis of the filter cake and standard cake mode filtration parameters. Detailed microstructural analysis was carried out to characterize the nature of IMCs captured in the filter cake. Fundamental cake filtration theory together with microstructural analysis of the filter cake can provide a quantitative measure for levels of IMCs present in the bath and overall metal cleanliness of the coating bath.

Keywords: *Pressure-filtration, Filter-cake, IMCs, Specific cake resistance, Filtration curve*

1. Introduction

Molten metal cleanliness is often assessed by chemical and detailed metallographic analyses. An inline and real-time analysis of the quality of melt in production lines has been a challenge in liquid metal processing [1,2]. There are now widely used inclusion detection systems available including the Porous Disc Filtration or preconcentration tests (PoDFA), and the Liquid Aluminium Inclusion Sampler (LAIS) [2]. The PoDFA and the LAIS are pressure filtration techniques where the pressure differential above the atmosphere across the filter medium forces molten metal through the filter medium while inclusions and oxides are collected above the filter medium forming what is referred to as the filter cake. Through detailed metallographic and chemical analyses, these methods can provide both quantitative and qualitative assessment of molten metal cleanliness. In previous studies we have used the LAIS unit to assess the level of suspended dross intermetallic compound particles in 55%Al-Zn metal coating bath [3]. The LAIS technique in combination with metallographic and chemical analyses of the cake zone can be used to estimate the level of suspended dross particles in the metal coating bath.

However, the reliance of these techniques on off-line metallographic and chemical analyses is a time-consuming process and there is a need for inline real time assessment of molten metal cleanliness. A portable instrument, known as Prefil Footprinter, based on the pressure filtration technique, has been recently introduced [1,4]. This pressure filtration techniques uses the flowrate of molten metal through a ceramic foam filter at constant pressure and temperature to measure the inclusion content of the melt.

During the test, the filtrate weight is continuously measured as a function of filtration time and the graph of the weight versus time is displayed on the data acquisition system monitor. The slope and the overall shape of the graph is used to assess the cleanliness of the melt: the cleaner the melt the higher the weight vs time curve will

†Corresponding author: Nega.Setargew@BlueScopesteel.com

be. On a contaminated melt, on the other hand, oxides, inclusion such as dross intermetallic compound particles (IMCs) are accumulated on the surface of the filter forming the filter cake which acts as a filter and reduces the flow rate of the melt. Comparing the graph of the filtrate weight versus the filtration time graph with a similar graph of a clean melt, gives a comparative measure for cleanliness of the melt in real-time.

In this paper we applied classical cake filtration theory to analyse the cumulative filtrate volume versus pressure filtration time data produced from the Prefil unit together with detailed metallographic characterization of the filter cake to estimate the IMCs captured/unit filtrate volume.

2. Cake Mode Filtration

2.1 Theoretical Cake Mode Filtration Considerations

The Prefil melt quality assessment and the production of concentrated inclusion samples for metallographic assessment is based on Darcy's Law and cake filtration principles. Cake filtration is one of the oldest unit operations in solid-liquid separation. Analysis of the filtration data using cake mode filtration principles will require calculations of the filter medium and the specific cake resistances taking into considerations the simultaneous processes of flow of liquid in the porous medium and the build-up of inclusions as the filter cake.

Since the specific cake resistance is one of the most important parameters in cake filtration, we will use the underlying governing equations based on Darcy's Law to quantify the solids content (IMCs and oxide inclusions) of the filter cake.

The cake filtration parameters are derived from Darcy's law for laminar, single-phase flow through a porous media. It relates the linear relationship between volumetric flow rate of the fluid q and the pressure gradient.

Rate of filtration =

$$\frac{\textit{The Driving force}(\textit{the pressure differential})}{\textit{Resistance}}$$

$$q = \frac{Ak\Delta p}{\mu \Delta x} \tag{1}$$

Where:

q the volumetric flow rate of the filtrate
μ the viscosity of the melt
A the cross-sectional area of the filter medium
Δp the applied pressure difference
k the permeability of the filter medium
Δx filter medium thickness

2.3 Generalized Equation- Cake Filtration

During filtration the filter medium resists the passage of the fluid under the pressure differential across the filter medium. The filter cake thickness increases with time as filtration progresses. The flow velocity is proportional to the pressure difference Δp imposed over the cake and the filter medium [4-6]. The fluid velocity is inversely proportional to the viscosity and the filter and cake resistance.

$$u = \frac{1}{A}\frac{dV}{dt} = \frac{\Delta p}{\mu(Rc + Rm)} \tag{2}$$

$$Rc = \alpha\sigma\frac{V}{A} \tag{3}$$

Substituting equation 3 into equation 2 we have:

$$\frac{dV}{dt} = \frac{\Delta p}{\frac{\mu}{A}\left(\alpha\sigma\frac{V}{A} + Rm\right)} \tag{4}$$

or

$$\frac{dt}{dV} = \frac{\mu\sigma\alpha}{A^2(\Delta p)}V + \frac{\mu Rm}{A(\Delta p)} \tag{5}$$

List of Symbols

A cross-sectional area of filter medium and cake, (m^2)
H cake thickness (m)
Δx_f, H_f Filter medium thickness (m)
Δx_c, H_c Filter cake thickness (m)
ΔP Pressure difference across cake and filter medium (Pa)
q Volumetric flow rate (dV/dt) ($m^3 \cdot s^{-1}$)
R_c Resistance of filter cake (m^{-1})
R_m Resistance of filter medium (m^{-1})
t Filtration time (s)
u Filtrate velocity ($m \cdot s^{-1}$)
V Volume of filtrate that has passed through the filter during time t (m^3)
W Weight of filtrate that has passed through the filter during time t (kg)

μ Viscosity of melt/filtrate (Pa·s or N·s·m^{-2})
α Specific cake resistance (m·kg^{-1})
ρ_{IMC} Density of IMC phase (kg·m^{-3})
ρ_f Density of filtrate (kg·m^{-3})
ρ_c Density of cake (kg·m^{-3})
σ Solid IMC mass captured per unit filtrate volume (kg·m^{-3})

Concentration factors:

K_H Proportionality volume of cake/volume of filtrate (m^3/m^3)
K_m Proportionality weight of cake /volume of filtrate (kg/m^3)

3. Experimental Methods

The pressure filtration experiments were carried out using 55%Al-Zn based coating metal from the Main pot (the coating bath) and the Premelt pot where Al-Si ingot and high-grade zinc ingots are melted and transferred to the main pot via a launder. The main difference between the Main and the Premelt pots is the iron content of the bath: the iron levels in the Premelt pot (at the process temperature of 600 ºC) is typically around 0.08 wt% whereas in the main pot the saturation Fe level for the coating alloy is around 0.42 wt%. However, due to the presence of suspended dross particles in the main pot, higher levels of iron can be expected.

In the filtration experiment we used a crucible fitted with a micro (an average pore size of 50 μm) ceramic foam filter with dimensions: Ø 7 mm diameter 6 mm height. The crucible was preheated for up to ~ 40 minutes and installed into the pressure chamber of the Prefil. After installing the crucible in the chamber, the melt in the sampling area was skimmed for ~ 5 minutes prior to sampling to remove the top dross on the surface of the melt. The surface of the melt was skimmed again ~ 1 minute before the ladle is immersed into the pot. The ladle was immersed to ~ 500 mm depth and a sample of the melt (~ 2 kg was poured into the pre-heated crucible in the test chamber. After pouring the melt, the lid of the chamber is closed and when the test temperature is achieved (595 ºC for the main pot and 630 ºC for the Premelt), a constant pressure 8.27×10^4 Pa (0.08 MPa) was applied in the test chamber forcing metal to flow through the porous micro-filter disc. The total duration of the filtration experiment was pre-set to 150 s. The weight of the filtrate was measured every 3 seconds using the load cell connected to the data acquisitions system of the Prefil unit. At the end of each experiment, the pressure was released from the pressure chamber the melt in the crucible including the filter cake and filter medium were cooled to room temperature and the filter cake and the medium are sectioned for metallographic and chemical analysis. The filter cake and the micro ceramic foam filter were sectioned in the longitudinal direction and one-half of the sample was used for chemical analysis by ICP and the second half of the filter cake was used for characterization of the microstructure of the filter cake.

4. Results and Discussion

4.1 Pressure filtration flow curves

As stated in the preceding sections, the assessment of the level of dross intermetallic compound particles (IMCs) in the Main coating pot was carried out by making a direct comparison of the flow curves of the Premelt pot and the Main pot. Since iron is continuously dissolving from the steel strip in the bath, excess iron above the solubility limit is converted to the IMC phase τ5c-Al20Fe5Si2 (+Zn) which is the phase that is in equilibrium with the coating bath. The amount of iron that dissolves from the strip and forms the suspended dross particles in the main pot depends on the process conditions. Process conditions including bath temperature, the line speed, the strip entry temperature, and changes in process conditions all contribute to the level of iron in the bath and ultimately to the level of suspended dross particles in the pot. Since the level of suspended dross is the major difference between the Premelt and the Main pots, a direct comparison can be made between a clean and a contaminated melt with respect to at least suspended IMC particles in the Main pot. The level of oxides in the premelt pot is expected to be slightly higher since the melt in the Premelt pot is operated at around 630 ºC.

For a melt free of inclusions, the cumulative weight vs time curve will be a linear plot. On the other hand, for a contaminated melt, as the number of inclusions gradually increase at the filter medium interface, the flow rate of the melt through the porous media will progressively

decrease and the curve will deviate from linearity and become parabolic with a reduced slope. The characteristic flow curves that can occur are shown in the schematic diagram in Fig. 1. A linear curve signifies a clean melt, and the parabolic curves represent the filtration behaviours of a melt with entrained oxide films, solid inclusion particles such as dross IMC particles. The presence of a combination of inclusions of oxide double films, and particulates in Prefil experiments is predicted to result in the complex truncated parabolic curve [7].

The cumulative filtrate weight of the Main pot and Premelt pot samples are plotted and are shown in Figs. 2a to 2e. The filter cakes from the Main Pot experiments were sectioned for chemical and metallographic analyses.

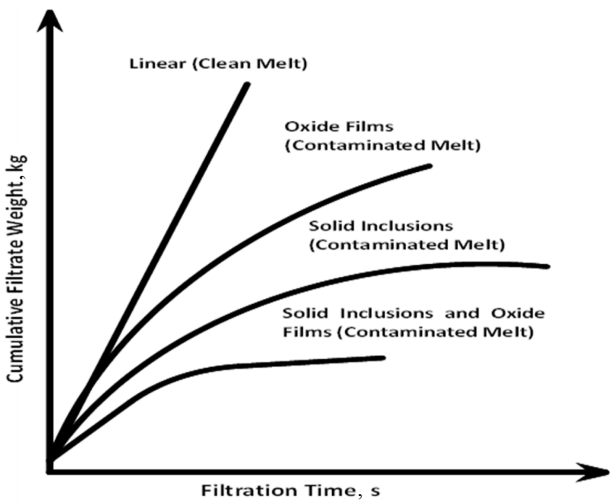

Fig. 1. Schematic diagram of the shapes of the Prefil curves and their interpretation [7].

Using the Fe content of the filter cake determined by ICP chemical analysis, the volume fraction IMC particles collected in the filter cake was estimated. In the calculation, the Fe content of τ5c-Al20Fe5Si2 (+Zn) IMC phase was set at 30-32 wt% [8]. The volume fraction of the IMC phase, V_f in the filter cake was calculated using Eq. 6. The density of the cake was estimated by a rule-of-mixtures approximation (Eq. 7) using 3550 kg/m^3 as the density of the IMC phase and 3304 kg/m^3 for the density of the melt at 600 ºC.

$$V_f = \frac{\frac{m_{IMC}}{\rho_{IMC}}}{\left[\frac{m_{IMC}}{\rho_{IMC}} + \frac{m_{melt}}{\rho_{melt}}\right]} \tag{6}$$

$$\rho_{cake} = Vf_{IMC} \cdot \rho_{IMC} + Vf_{melt} \cdot \rho_{melt} \tag{7}$$

In Table 1 are shown the process lines speeds, the iron content of the filter cake, and the estimated volume fractions of the IMCs in the filter cake for the main pot samples. Table 2 shows the total weight of the filtrate for the filtration time of 147 seconds for both the Premelt and Main pot samples.

The Prefil experiments were conducted during the processing of the commercial quality (CQ) and the full hard (FH) grades. The CQ grades were processed at lower line speeds than the FH samples (Table 1). The strip entry temperatures for both groups were identical whilst the strip residence time in the coating pot for the CQ grades

Table 1. Cumulative filtrate weight of the premelt and main pot samples (kg).

Sample	Product Grade	Line Speed (m/min)	Fe (wt%)	Volume Fraction of IMCs in Cake (%)	Cake Thickness (mm)
Main Pot -1	CQ	116	7.6	24	5.0
Main Pot -2	FH	136	1.7	5.2	1.6
Main Pot -3	CQ	108	2.2	6.8	2.0
Main Pot- 4	FH	127	1.8	5.6	1.3
Main Pot- 5	CQ	108	1.6	4.9	1.8

Table 2. Cumulative filtrate weight of the premelt and main pot samples (kg)

Pot	Sample 1-CQ	Sample 2-FH	Sample 3-CQ	Sample 4-FH	Sample 5-CQ
Premelt Pot	1.88	1.30	1.44	1.15	1.47
Main Pot	1.16	0.96	1.02	1.00	0.93

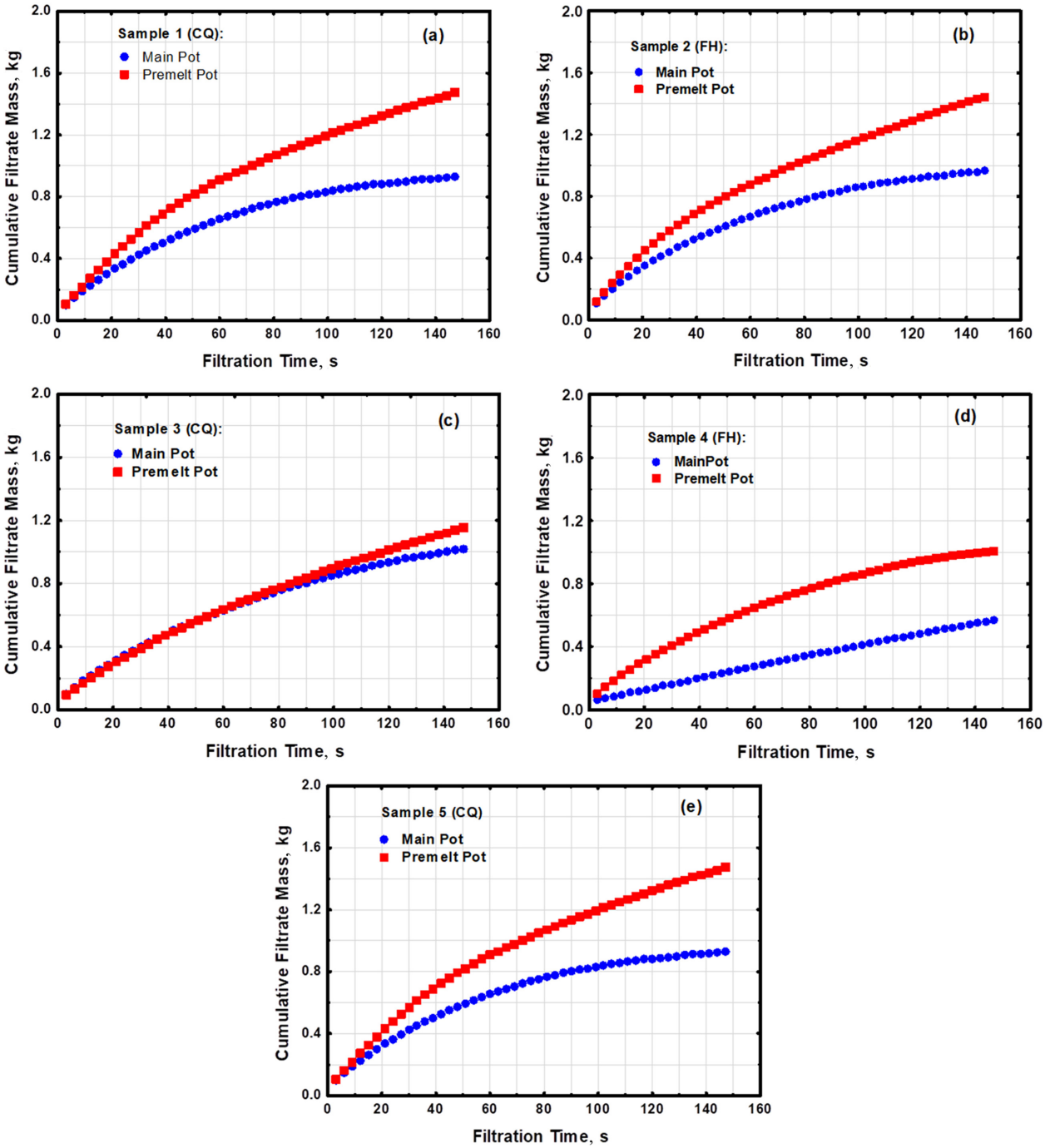

Fig. 2. The flow curves of Main and Premelt samples: (a) 1-CQ, (b) 2-FH, (c) 3-CQ, (d) 4-CQ and (e) 5-FH.

were longer than for the FH grades.

As shown in Figs. 2, the flow curves for both the main and premelt pot samples are parabolic with significantly higher differences in the slope of the curves between the premelt and main pot samples except in sample 3-CQ, (Fig. 2c) where both the main and premelt pots curves coincided and displayed identical filtration behaviour for up to ~ 60% of the duration of the filtration experiment.

Sample 1-CQ showed the highest difference in the slope of the flow curve between the clean (Premelt pot) and Main pot (Fig. 2a) followed by sample 5 (Fig. 2e). Similarly, samples 3 (Fig. 2c) showed higher slope than sample 2 (Fig. 2b). Comparison of the premelt and main pot shows differences in metal flow rates between the CQ

and FH samples. The CQ samples had higher residence time in the pot (lower line speed) than the FH samples processed at higher line speed and lower residence times. This may be attributed to the precipitation of dross intermetallic particles due to higher dissolution rate of the strip and the long residence of the strip in the bath compared to the FH samples that had shorter residence time in the pot. While the flow curves can be used for qualitative assessment of the level of dross particles in the main pot, one of the major advantages of the Prefil pressure filtration technique is its ability to produce a highly concentrated filter cake sample from a melt with very low

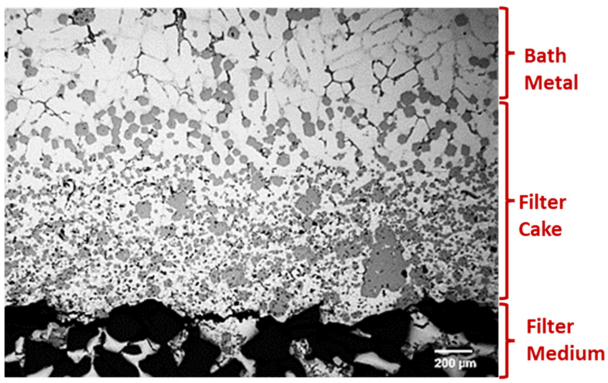

Fig. 3. Cross-section of the filter cake showing the area of the chemical analysis (labelled filter cake).

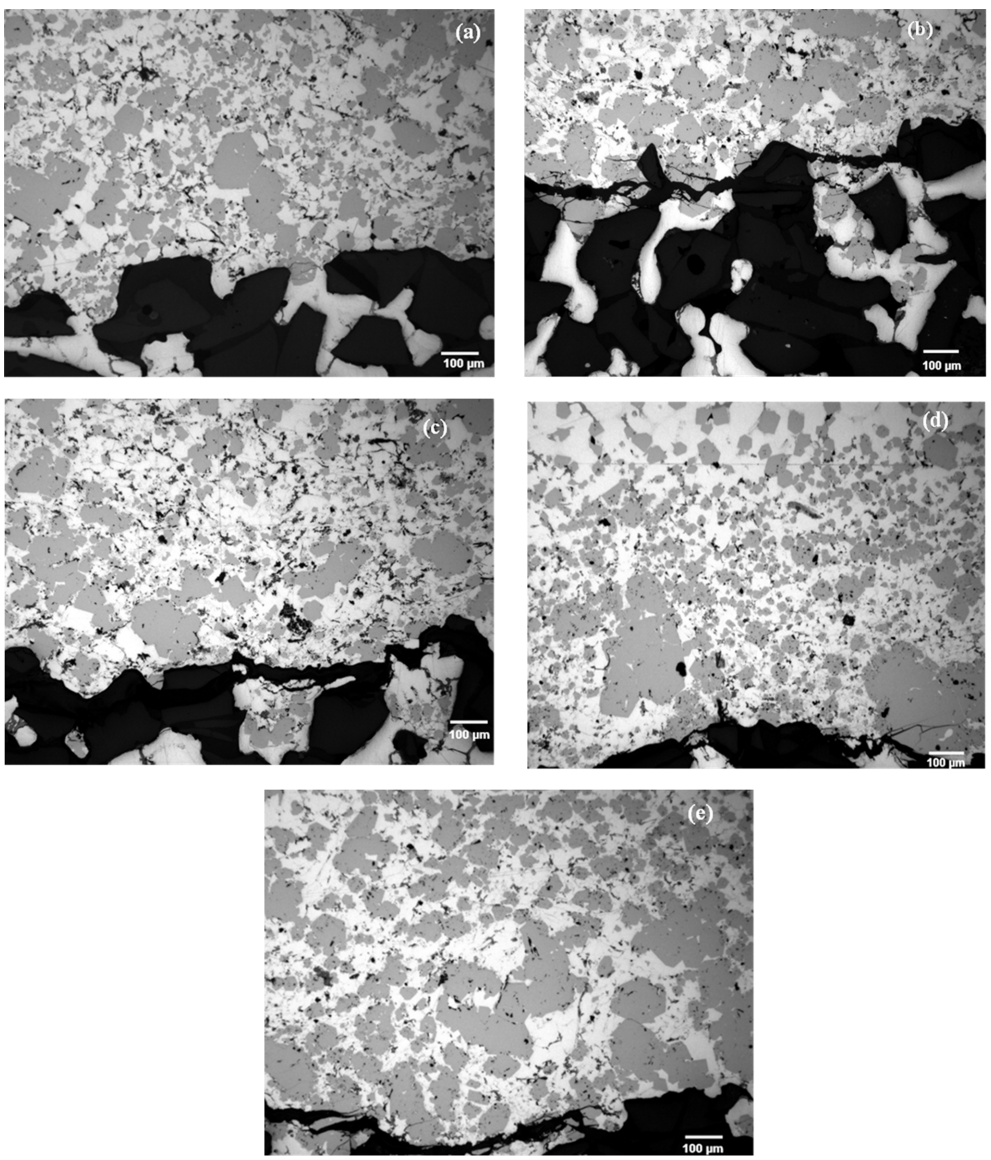

Fig. 4. The microstructure of the filter cake showing the size and morphology of the IMCs collected in the filter cake in samples: (a) Sample 1-CQ, (b) Sample 2-FH, (c) Sample 3-CQ, (d) Sample 4-FH and (e) Sample 5-CQ.

inclusion content. This enables a more comprehensive, quantitative analysis of the melt's inclusion content. Fig. 3 illustrates the specific regions in a typical pressure filtration sample: the bath metal above the filter cake, the filter cake with its agglomerated IMCs, and the ceramic filter medium. The chemical analysis of each of the samples was carried out in the region labelled Filter Cake (Fig. 3).

Figs. 4a to 4e show the microstructures of the centre regions of the filter cake samples from the Main pot. Even though, the amount of suspended dross particles in the melt is quite low (typically 0.03 to 0.04 wt%), highly concentrated samples of filter cakes were produced. The IMCs in the filter cake (Figs. 4) show particle sizes ranging from a few microns to agglomerated clusters of IMCs ranging from tens to more than hundreds of microns in size.

The range of particle sizes observed except for the larger agglomerated clusters, can be expected to remain suspended in the bath since settling in a gravitational field is largely driven by the density difference between the dross particles and the melt. The settling velocity, V_s, is given by a balance of the buoyant and the drag forces (Eq. 8). Where $\Delta\rho$ is the density difference between the inclusion and the melt, d is the inclusion diameter and g is the acceleration due to gravity, 9.8 m/s^2, and μ is the viscosity of the melt [5]. It can be shown that the settling velocities are extremely slow, for example the settling velocity of a 100 μm diameter particle in a quiescent melt is estimated to be around 800 μm/s similarly a 20 μm particle will settle at around 30 μm/s. For non-spherical particles or suspensions settling velocities will be significantly reduced due to increased drag forces and the effects of volume fractions of inclusions. While in a contaminated melt with high volume fractions of suspended dross particles, some inferences can be made directly from the Fe content of the bath, the pressure filtration technique has the added advantage of providing both the flow curves and producing a concentrate of the fine suspended IMCs and the agglomerated clusters of dross particles collected per kg of the melt filtered (IMCs/kg).

$$V_s = \frac{\Delta\rho d^2 g}{18\mu} \tag{8}$$

In the interpretation of the microstructure of the cake it should be noted that size of the IMCs can be affected by the diffusion of Fe in solution in the melt as solidification progresses since the solubility of Fe in the solid phase is of the order of < 0.02 wt%. The IMCs in the filter cake are therefore likely to grow as solidification progresses with the Fe in solution diffusing to the pre-existing IMC particles acting as the sink for Fe. In a related thermal analysis study conducted under a similar prefil test configuration, we showed that it will take approximately 30 minutes before the formation of solid α-Al phase begins in 55%Al-Zn alloy (liquidus temperature: 557 ºC).

This will provide sufficient time for agglomeration and clustering of fine dross IMC particles by Ostwald ripening to large particles of IMCs in the filter cake. The dominant mechanism for particle growth is most likely a combination of Ostwald ripening and agglomeration and clustering of the IMC particles in the filter cake. This is clear in the micrographs the filter cakes of all the samples examined. Overall, the larger sizes of IMCs occupy the lower half (close to the filter cake – ceramic filter interface).

4.2 Application of Cake Mode Filtration Model to the Prefil Pressure Filtration Results

In conventional cake filtration theory, the cumulative resistance to filtration is a sum of the resistance encountered within the filter cake and the inherent resistance presented by the filter medium. The experimental results are plotted in the form: inverse

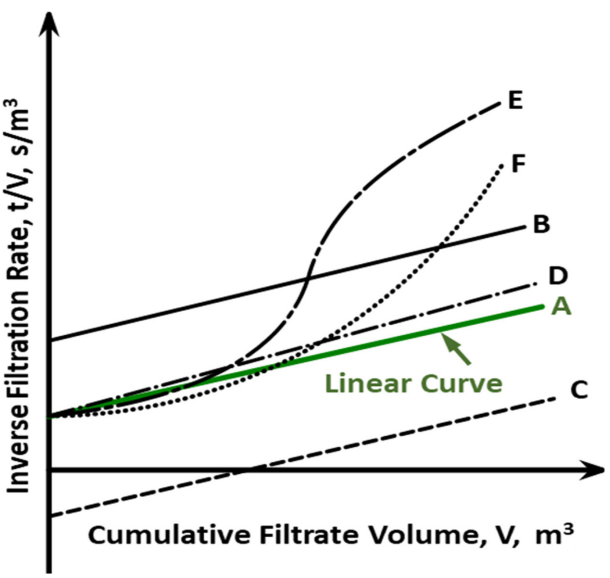

Fig. 5. Schematic diagram showing deviation from linearity of the inverse filtration rate t/V vs V [10].

filtration rate t/V as a function the cumulative filtrate volume, V resulting in the well-known linear equation which is used for determining the resistance parameters in constant pressure filtration. To show deviations from linearity due to secondary effects, the instantaneous resistance to flow is plotted as a function of the quantity filtered (equation (4) and equation (5)).

In constant pressure filtration, t/V vs V plot should be a straight line provided the data is not affected by secondary effects [4,9]. Where $\mu Rm/A(\Delta p)$ in equation

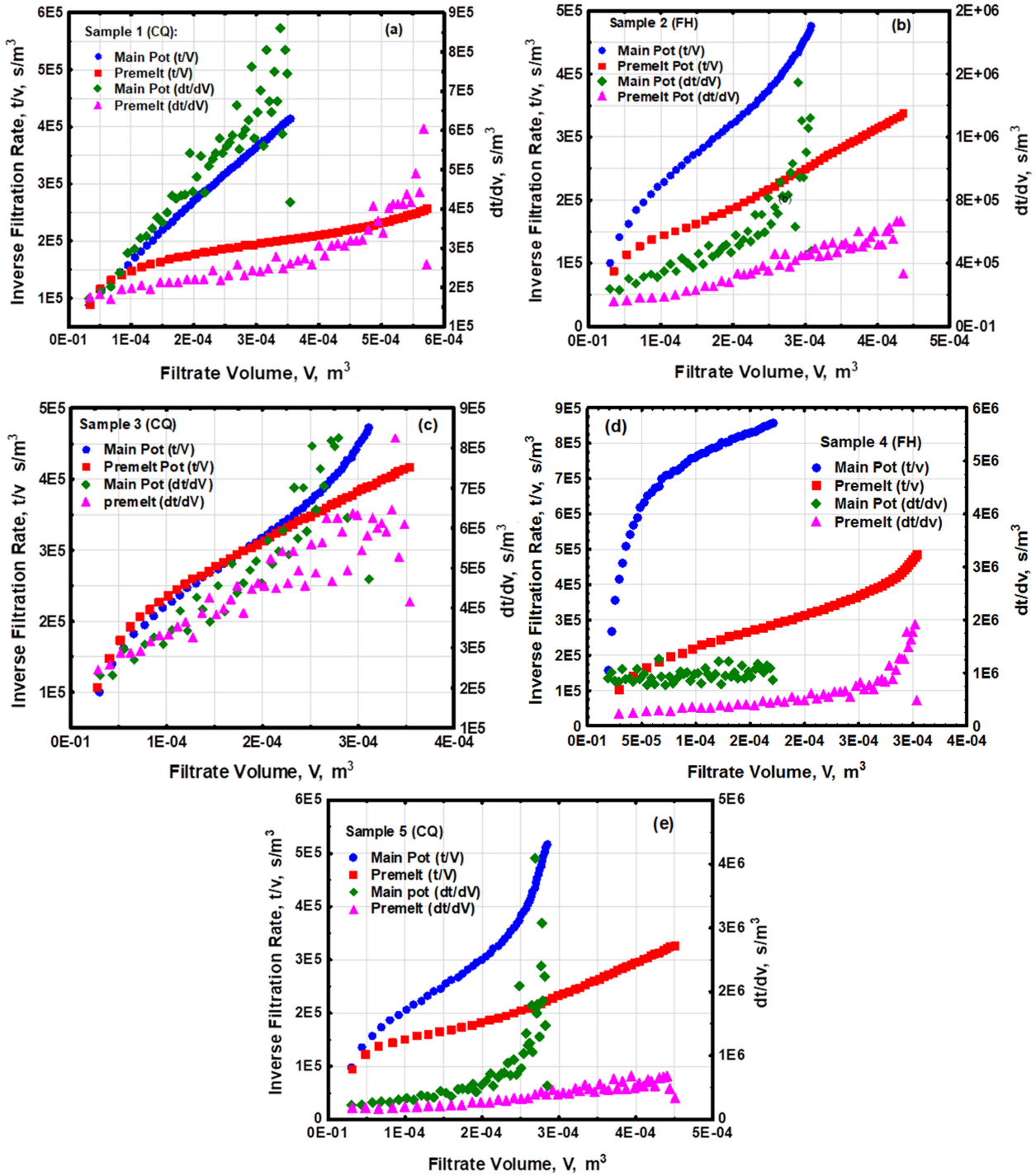

Fig. 6. Inverse filtration rate, t/V and dt/dV plots showing the deviations from linearity due to secondary effects: (a) Sample 1-CQ, (b) Sample 2-FH, (c) Sample 3-CQ, (d) Sample 4-FH and (e) Sample 5-CQ.

(5) is obtained from the intercept line with the t/v-axis, while the slope gives $\mu\sigma\alpha/A^2(\Delta p)$. The data of the pressure filtration experiments are summarized in Figs. 6a to 6e which show the t/V-V and the dt/dV-V plots. In constant pressure filtration, t/v vs V plot should be a straight line. Where $\mu Rm/A(\Delta p)$ in equation (5) is obtained from the intercept line with the t/v-axis, while the slope gives $\mu\sigma\alpha/A^2(\Delta p)$.

The data of the pressure filtration experiments are summarized in Figs. 6a to 6e which show the t/V-V and the dt/dV-V. Theoretically the inverse filtration plots (t/V-V and dt/dV-V) are expected to produce linear plots assuming the data remains unaffected by secondary influences which would result in deviation from linearity. The factors responsible for deviations from linearity in the t/V-V and dt/dV-V plot as defined in the German Standard VDI 2762 Part 2 are described using the schematic diagram shown in Fig. 5 [10]. The linear curve, A in Fig. 5 depicts the theoretical curve without secondary effects. B: signifies solids settling before the start of filtration (increasing the filter medium resistance). C: the starting point of filtration was not measured. D: solids settle out completely increasing the cake growth rate. E: only coarse particles settle. After some time only the remaining fines are filtered, and the resistance increases progressively. F: fine particles trickle through the cake or the filter medium. In contrast to the flow curves shown in the preceding sections in Fig. 2, the slopes in the inverse filtration rate, t/V and dt/dV curves have higher slope for melts with higher volume fractions of IMCs and entrained dispersions oxide particles. For sample 1-CQ, the t/V and the dt/dV plots display higher slopes signifying the high volume fractions of IMCs present in the sample. The premelt t/V and dt/dV curves, on the other hand, show significantly lower slopes but there is evidence of deviations from linearity most likely due to the trickling effect of dispersions of oxide particles in the premelt sample. In sample 2-FH, the t/V plot has higher slope the premelt due to the level of IMCs in the main pot sample. The main pot dt/dv plot shows significant deviations due to particles trickling and blocking the pores of the cake or the filter medium. This is consistent with the micrograph shown in Fig. 4b where there is clear evidence of IMC occupying the entire filter web shown in the right-hand corner in the figure. But there were no significant deviations displayed in the dt/dV plot of the premelt sample. In Sample 3 (Fig. 6c), the t/V plots of both the main and premelt pot demonstrated strikingly similar slopes for approximately 60% of the filtration time, corresponding closely with the findings from the cumulative mass flow rate vs filtration time plots in Fig. 2c. However, the dt/dV plots for both main and premelt pot samples show significant scatter and more deviations from linearity in the main pot sample. The main pot t/V plot of sample 4-FH showed pronounced deviations from linearity and exhibited a rapid increase is most likely related to large particles settling and blocking the pores of the filter medium. This was also reflected in the dt/dV plot where dt/dV plot remained constant signifying the rapid increase and a constant flow resistance. The premelt plots of t/V and dt/dV remained largely linear with deviations appearing towards the end of the filtration time. Sample 5-CQ showed characteristic deviation resulting from both blockage of the pores in the filter cake and the filter medium. This is clearly shown in the steep increase in the resistance of overall filtration shown in the t/V and dt/dV plots of the Main pot samples while for the Premelt samples there was a slight deviation in t/V plot and the dt/dV plot remained linear.

4.3 Estimation of the Cake Mode Filtration Parameters

The filter cake and filter medium resistance and more importantly the mass of dross particles collected per unit filtrate volume filtered were calculated using the proportionality factors: volume cake/volume of filtrate, K_H (m^3/m^3) and the mass of cake/volume of filtrate K_m (kg/m^3) using equation 9 and 10 [9].

$$K_H = \frac{A \cdot H}{V} \tag{9}$$

$$K_m = \frac{m}{V} \tag{10}$$

$$R_c = \alpha\frac{\Delta P \cdot A}{\mu} \tag{11}$$

$$\alpha_H = b\frac{A^2 \cdot \Delta P}{K_H\mu} \tag{12}$$

$$\alpha_M = b\frac{A^2 \cdot \Delta P}{K_M\mu} \tag{13}$$

Table 3. Properties used to calculate the cake filtration parameters.

Parameter	Value
Pressure drops across cake and filter medium, ΔP (Pa)	8.27×10^{4}
Density of IMC phase (kg/m^3)	3550
Density of melt at 600 °C (kg/m^3)	3304
Density of cake (rule-of-mixture approximation (kg/m^3)	3363
Filter medium cross sectional area, A (m^2)	3.85×10^{-5}
Viscosity of melt, μ (Pa·s)	1.65×10^{-3}

Table 4. Estimates of the cake mode filtration parameters for the Main pot samples 1-5.

Parameter	Unit	Sample 1	Sample 2	Sample 3	Sample 4	Sample 5
IMC mass captured/unit filtrate volume	kg/m^3	4.7×10^{-1}	4.0×10^{-2}	6.1×10^{-2}	3.3×10^{-2}	4.4×10^{-2}
Volume cake/volume filtrate, KH	m^3/m^3	5.5×10^{-4}	2.1×10^{-4}	2.5×10^{-4}	1.65×10^{-4}	2.5×10^{-4}
Mass of cake/volume of filtrate, Km	kg/m^3	1.84	7.0×10^{-1}	8.3×10^{-1}	5.5×10^{-1}	8.15×10^{-1}
Filter medium resistance, Rm	m^{-1}	1.9×10^{11}	3.9×10^{11}	3.9×10^{11}	3.9×10^{11}	3.9×10^{11}
Filter cake resistance, Rc	m^{-2}	8.0×10^{14}	2.5×10^{14}	2.0×10^{14}	3.1×10^{14}	2.2×10^{14}
Cake resistance relative to cake thickness, α_H	m^{-2}	2.7×10^{14}	7.0×10^{14}	5.9×10^{14}	9.0×10^{14}	6.0×10^{14}
Cake resistance relative to mass of IMCs in cake, α_m	m/kg	8.0×10^{10}	2.1×10^{11}	1.8×10^{11}	2.7×10^{11}	1.8×10^{11}

In Table 4 are shown the key filter cake and filter medium resistance, Rc, the cake resistance relative to cake thickness, α_H and the cake resistance relative to the IMC and oxide inclusions (m/kg). The resistances were calculated using the parameters shown in Table 3 and Eqs. 11-13 and the slopes (b) and intercepts of the t/V and dt/dV plots of Eq. (5). The calculated values the filtration parameters are summarized in Table 4.

5. Conclusions

Based on the key findings of this work we make the following conclusions:

1. The Prefil pressure filtration technique enables real-time, semi-quantitative analysis of inclusion content and assessment of molten metal cleanliness. The shape of the fluidity curve, representing the flow rate of a predetermined amount of metal poured into a test crucible can directly be compared with previous benchmarks to give a measure of the cleanliness of the melt.
2. The Prefil data can be analysed using standard cake mode filtration principles to provide a precise quantitative evaluation of molten metal cleanliness.
3. From the inverse filtration rate (t/v) vs cumulative filtrate volume, V and dt/dV vs V a quantitative measure of the mass of inclusions content per unit volume of filtrate can be calculated.
4. Plotting t/V vs V and dt/dV vs V, can show the deviations from linearity compared with flow curves from the Prefil unit. The inverse plots show the filter cake formed is compressible and highlight the influence of secondary effects that need to be considered in the analysis.

Acknowledgement

We would like to thank many of our colleagues at BlueScope Innovation Labs for engaging discussions of this work and BlueScope Steel for permission to publish this work.

References

1. P. G. Enright, and I. R. Hughes, A Shop Floor Technique for Quantitative Measurement of Molten Metal Cleanliness of Aluminium Alloys, *Foundryman Magazine*, pp. 390 - 395, IBF Publications, Birmingham, UK (1996).
2. S. W. Hudson, and D. Apelian, Inclusion Detection in

Molten Aluminium Alloys, *International Journal of Metalcasting,* **10**, 289 (2016). Doi: https://doi.org/10.1007/s40962-016-0030-x

3. N. Setargew, D. J. Willis, D. Thompson, Detection of Dross Intermetallic Compound Particles in 55%Al-Zn Melt Using LAIS, *InterZAC2004*, pp. 1 – 16, Seoul, Korea (2004).
4. X. Cao, Filtration Resistance During Pressure Filtration Tests of Liquid Aluminium Alloys, *International Journal of Materials Research*, **97**, 1163 (2006). Doi: https://doi.org/10.1515/ijmr-2006-0183
5. T. A. Engh, C. J. Simensen, and O. Wijk, *Principles of Metal Refining*, *1st ed.*, p. 253, Oxford University Press (1992). Doi: https://doi.org/10.1093/oso/9780198563372.001.0001
6. M. Hennemann, M. Gastl and T. Becker, Influence of particle size uniformity on the filter cake resistance of physically and chemically modified fine particles, *Separation and Purification Technology*, **272**, 118966 (2021). Doi: https://doi.org/10.1016/j.seppur.2021.118966
7. A. M. Samuel, F. H. Samuel, H. W. Doty, and S. Valtierra, Inclusion Measurement in Al-Si Foundry Alloys Using Qualiflash and Prefil Filtration Techniques, *International Journal of Metalcasting,***12**, 625 (2018). Doi: https://doi.org/10.1007/s40962-017-0185-0
8. N. Setargew, D. J. Willis and A. Dixon, *Proc. 12th Int. Conf. on Zinc & Zinc Alloy Coated Steel Sheet (Galvatech 2021)*, pp. 1292 - 1301, Voestalpine Stahl GmbH, Vienna Austria (2021).
9. S. Ripperger, W. Gosele, and C. Alt, *Filtration, 1. Fundamentals Ullmann's Encyclopaedia of Industrial Chemistry*, **14**, 678 (2012). Doi: https://doi.org/10.1002/14356007.b02_10.pub2
10. VDI 2762 Part 2, German Standard, Mechanical Solid Liquid Separation, GVC (2010). https://www.vdi.de/fileadmin/pages/vdi_de/redakteure/richtlinien/inhaltsverzeichnisse/1717392.pdf